ResearchGate

See discussions, stats, and author profiles for this publication at: https://www.researchgate.net/publication/317586900

Band alignment of atomic layer deposited SiO 2 and HfSiO 4 with $(\bar{2}01)$ β-Ga 2 O 3

Article *in* Japanese Journal of Applied Physics · July 2017
DOI: 10.7567/JJAP.56.071101

CITATIONS
2

READS
35

7 authors, including:

Patrick Carey
University of Florida
9 PUBLICATIONS **19** CITATIONS
SEE PROFILE

Fan Ren
University of Florida
1,054 PUBLICATIONS **19,453** CITATIONS
SEE PROFILE

David C. Hays
University of Florida
63 PUBLICATIONS **503** CITATIONS
SEE PROFILE

Sang-Phil Jang
Catholic University of Korea
113 PUBLICATIONS **671** CITATIONS
SEE PROFILE

Some of the authors of this publication are also working on these related projects:

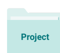

AlGaN/GaN Bio-Semsor View project

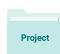

Compound semiconductor reliability and proton irradiation View project

All content following this page was uploaded by Patrick Carey on 08 October 2017.

The user has requested enhancement of the downloaded file.

IOPscience iopscience.iop.org

Home Search Collections Journals About Contact us My IOPscience

Band alignment of atomic layer deposited SiO_2 and $HfSiO_4$ with $(\bar{2}01)$ β-Ga_2O_3

This content has been downloaded from IOPscience. Please scroll down to see the full text.

2017 Jpn. J. Appl. Phys. 56 071101

(http://iopscience.iop.org/1347-4065/56/7/071101)

View the table of contents for this issue, or go to the journal homepage for more

Download details:

IP Address: 128.227.249.21
This content was downloaded on 14/06/2017 at 12:53

Please note that terms and conditions apply.

Japanese Journal of Applied Physics 56, 071101 (2017)
https://doi.org/10.7567/JJAP.56.071101

REGULAR PAPER

Band alignment of atomic layer deposited SiO_2 and $HfSiO_4$ with $(\bar{2}01)$ β-Ga_2O_3

Patrick H. Carey, IV[1], Fan Ren[1], David C. Hays[2], Brent P. Gila[2], Stephen J. Pearton[2*], Soohwan Jang[3], and Akito Kuramata[4,5]

[1]Department of Chemical Engineering, University of Florida, Gainesville, FL 32611, U.S.A.
[2]Department of Materials Science and Engineering, University of Florida, Gainesville, FL 32611, U.S.A.
[3]Department of Chemical Engineering, Dankook University, Yongin, Gyeonggi 16890, Korea
[4]Tamura Corporation, Sayama, Saitama 350-1328, Japan
[5]Novel Crystal Technology, Inc., Sayama, Saitama 350-1328, Japan

*E-mail: spear@mse.ufl.edu

Received April 14, 2017; accepted May 8, 2017; published online June 14, 2017

The valence band offset at both SiO_2/β-Ga_2O_3 and $HfSiO_4$/β-Ga_2O_3 heterointerfaces was measured using X-ray photoelectron spectroscopy. Both dielectrics were deposited by atomic layer deposition (ALD) onto single-crystal β-Ga_2O_3. The bandgaps of the materials were determined by reflection electron energy loss spectroscopy as 4.6 eV for Ga_2O_3, 8.7 eV for Al_2O_3 and 7.0 eV for $HfSiO_4$. The valence band offset was determined to be 1.23 ± 0.20 eV (straddling gap, type I alignment) for ALD SiO_2 on β-Ga_2O_3 and 0.02 ± 0.003 eV (also type I alignment) for $HfSiO_4$. The respective conduction band offsets were 2.87 ± 0.70 eV for ALD SiO_2 and 2.38 ± 0.50 eV for $HfSiO_4$, respectively.
© 2017 The Japan Society of Applied Physics

1. Introduction

The commercial availability of high quality, large diameter Ga_2O_3 single-crystals and wide bandgap of this material make it a very promising material for high power electronic devices and solar-blind UV photodetectors used for various military and commercial applications.[1–13] The β-polymorph has a higher theoretical breakdown field than both GaN and SiC, although significant hurdles remain in overcoming its low thermal conductivity.[4,6,7] Promising device performance has been reported for rectifiers, transistors and solar-blind photodetectors on bulk, epitaxial and thin flakes of β-Ga_2O_3.[4–13] There is a need for dielectric/Ga_2O_3 combinations that can be used as gates on metal–oxide–semiconductor (MOS) transistors, as well as passivation layers to prevent surface conductivity changes common to electronic oxides exposed to humid ambients.[4,6] The gate dielectrics reported for β-Ga_2O_3 have typically been either atomic layer deposited (ALD) Al_2O_3 or HfO_2 or ALD and plasma enhanced chemical vapor deposited (PECVD) SiO_2.[14–21] The wide bandgap of Ga_2O_3 limits the choices than can potentially achieve the >1 eV conduction and valence band offsets preferred for MOS transistors.

Kamimura et al.[16] measured the conduction and valence band offsets of Al_2O_3 with β-Ga_2O_3 as 1.5 ± 0.2 eV and 0.7 ± 0.2 eV, respectively. Hattori et al.[17] measured conduction and valence band offsets of 1.9 and 0.5 eV, respectively for high quality epitaxial films of γ-Al_2O_3 on single-crystal Ga_2O_3. Konishi et al.[15] obtained a conduction band offset of 3.1 ± 0.2 eV and valence band offset of 1.0 ± 0.2 eV for the SiO_2/β-Ga_2O_3 interface when the SiO_2 was deposited by PECVD. However, Jia et al.[14] got a much smaller valence band offset (0.43 eV) measured with X-ray photoelectron spectroscopy (XPS) for SiO_2 deposited by ALD on single crystal β-Ga_2O_3, with a corresponding larger conduction band offset of 3.63 eV. Wheeler et al.[18] measured the band alignment between ALD ZrO_2 or HfO_2 and β-Ga_2O_3 and both dielectrics resulted in a type II, staggered gap alignment with a conduction band offset of 1.2 and 1.3 eV for ZrO_2 and HfO_2 films, respectively. Table I provides a summary of reported values of band offsets and alignment type for dielectrics on β-Ga_2O_3. Please note that in some cases the β-Ga_2O_3 was either amorphous or polycrystalline and thus interface states may place a role in band alignments in those cases. There is typically variability reported in the literature for both valence and conduction band offsets due to various effects.[22,23] Some of these effects include metal contamination in the deposited dielectric (especially in sputtered films), interface disorder, differences in dielectric composition as a result of different deposition methods or precursors, carbon/hydrogen contamination, annealing, stress/strain and type of surface termination.[23] In some cases, these result in differences in the bandgap of the dielectric and thus affect the conduction band offset. Generally, the valence band offset is measured directly and the conduction band offset calculated from the difference between that and the bandgaps. However, the valence band offset can also be affected by most of these same issues. The use of ALD deposited dielectrics minimizes most of these effects and provides a more controlled method for making the heterostructure samples need to determine the band alignment.

In this paper, we report on the determination of the band alignment in the SiO_2/β-Ga_2O_3 and $HfSi_2O_4$/β-Ga_2O_3 heterostructures, in which both the dielectrics were deposited by ALD. While SiO_2 band offsets with Ga_2O_3 have been measured for both ALD and PECVD SiO_2, there is significant variability in the results reported to date and it is worth making additional studies to clarify the more usual values. In addition, $HfSiO_4$ has a significantly higher dielectric constant than SiO_2, allowing for thicker films with equivalent capacitance and advantages in terms of MOS device applications. Thus it is also worth examining the band offsets of this dielectric with β-Ga_2O_3. We employ XPS[24,25] to determine the valence band offsets and by measuring the respective bandgaps of the SiO_2 (8.7 eV), $HfSiO_4$ (7.0 eV), and β-Ga_2O_3 (4.6 eV),[26] we were also able to determine the conduction band offset in the heterostructures and determine the band alignment.

2. Experimental methods

The SiO_2 and $HfSiO_4$ were deposited by ALD on Ga_2O_3 and quartz substrates. The latter were used for dielectric constant and composition measurements. Both thick (200 nm) and thin (1.5 nm) layers of the dielectrics were deposited to be able to measure both bandgaps and core levels on the β-Ga_2O_3. The

© 2017 The Japan Society of Applied Physics

Table I. Reported values for band offsets for different materials on Ga_2O_3.

Dielectric material (crystalline nature of Ga_2O_3)	Synthesis method	ΔE_C (eV)	ΔE_V (eV)	Alignment type	Reference
SiO_2 (single crystal)	PECVD	3.1 (±0.2)	1.0 (±0.2)	I	15
SiO_2 (single crystal)	ALD	3.63–3.76	0.3–0.43	I	14
SiO_2 (single crystal)	ALD	2.9 (±0.7)	1.2 (±0.2)	I	This work
Al_2O_3	ALD	1.5–1.6 (±0.2)	0.7 (±0.2)	I	16
γ-Al_2O_3 (single crystal)	PLD	1.9	0.5	I	17
Al_2O_3 (single crystal)	ALD	2.23 (±0.2)	0.07 (±0.2)	I	36
Al_2O_3 (single crystal)	PVD	3.16 (±0.2)	−0.86 (±0.2)	II	36
Si (amorphous)	PLD	−0.2 (±0.1)	−3.5 (±0.1)	I	21
GaN (polycrystalline)	Oxidation	−0.1 (±0.08)	−1.4 (±0.08)	I	19
6H-SiC (amorphous)	PVD	0.89 (±0.1)	−2.8 (±0.1)	II	20
ZrO_2 (single crystal)	ALD	1.2	−0.3 (±0.04)	II	18
HfO_2 (single crystal)	ALD	1.3	−0.5 (±0.04)	II	18
$HfSiO_4$ (single crystal)	ALD	2.38 (±0.5)	0.02 (±0.003)	I	This work

ALD layers were deposited at 200 °C in a Cambridge Nano Fiji 200. The ternary films were made by depositing alternating cycles of HfO_2 and SiO_2 to achieve the $HfSiO_4$ composition.[22] All layers were deposited using remote plasma atomic layer deposition using an inductively coupled plasma (ICP) source at 300 W. Plasma mode ALD helps lower contaminants in the film and reduces the nucleation delay while minimizing ion induced damage by utilizing a remote source. The $HfSiO_4$ precursors were tetrakis(dimethylamido)-hafnium(IV) and O_2 and resulted in a deposition rate of 0.9 A/cycle.[22] Likewise, the SiO_2 layers were deposited using precursors of tris(dimethylamino)silane and O_2, and produced a deposition rate of 0.63 A/cycle. Plasma mode ALD helps lower contaminants in the film and reduces the nucleation delay while minimizing ion induced damage by utilizing a remote source. The bulk β-phase Ga_2O_3 single crystals with ($\bar{2}01$) surface orientation (Tamura) were grown by the edge-defined film-fed growth method. Hall effect measurements showed the sample was unintentionally n-type with an electron concentration of $\sim 3 \times 10^{17}\,cm^{-3}$. The samples were not exposed to air prior to the subsequent XPS measurements to avoid complications from surface contamination. The latter may lead to less accurate band gap measurements when using reflection electron energy loss spectroscopy.

To obtain the valence band offsets, XPS survey scans were performed to determine the chemical state of the SiO_2, $HfSiO_4$ and β-Ga_2O_3 and identify peaks for high resolution analysis.[24,25] A Physical Electronics PHI 5100 XPS with an aluminum X-ray source (energy 1486.6 eV) with source power 300 W was used, with an analysis area of $2 \times 0.8\,mm^2$, a take-off angle of 50° and an acceptance angle of ±7°. The electron pass energy was 23.5 eV for the high resolution scans and 187.5 eV for the survey scans. The approximate escape depth ($3\lambda \sin\theta$) of the electrons was 80 Å. All of the peaks are well-defined in this system.

Charge compensation was performed using an electron flood gun. The charge compensation flood gun is often not sufficient at eliminating all surface charge, and additional corrections must be performed. Using the known position of the adventitious carbon (C–C) line in the C 1s spectra at 284.8 eV, charge correction was performed. During the measurements, all the samples and electron analyzers were electrically grounded so they were performed providing a common reference Fermi level. Differential charging is a serious concern for photoemission dielectric/semiconductor band offset measurements.[22,25] While the use of an electron flood gun does not guarantee that differential charging is not present and in some cases could make the problem worse, our experience with oxides on conducting substrates has been that the differential charging is minimized with the use of an electron gun. Calibrations with and without the gun and verified that was the case. This procedure has been described in detail previously.[22,26]

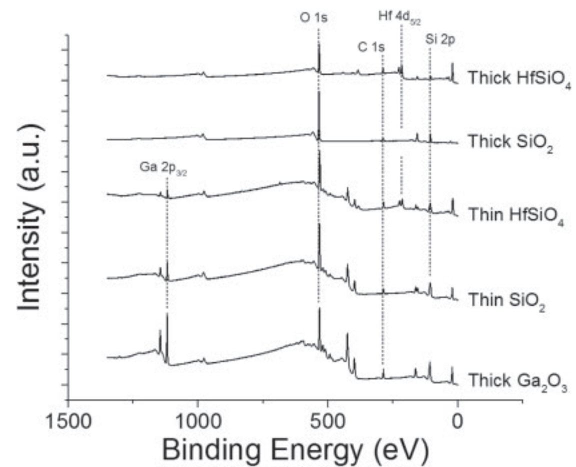

Fig. 1. XPS survey scans of thick ALD SiO_2 on bulk β-Ga_2O_3 and thick $HfSiO_4$ on bulk β-Ga_2O_3, thin (1.5 nm) ALD SiO_2 and $HfSiO_4$ on bulk β-Ga_2O_3 and the β-Ga_2O_3 bulk sample by itself. The intensity is in arbitrary units (a.u.).

Reflection electron energy loss spectroscopy (REELS) was employed to measure the bandgaps of the SiO_2, $HfSiO_4$ and β-Ga_2O_3.[17] REELS is a surface sensitive technique capable of analyzing electronic and optical properties of ultrathin gate oxide materials because the low-energy-loss region reflects the valence and conduction band structures.[26] It has been successfully used previously in conjunction with photoemission spectroscopy to measure band-alignment of γ-Al_2O_3/β-Ga_2O_3.[17] REELS spectra were obtained using a 1 kV electron beam and the hemispherical electron analyzer.

3. Results and discussion

Figure 1 shows the stacked XPS survey scans of thick (200 nm) SiO_2 and $HfSiO_4$, 1.5 nm ALD SiO_2 or $HfSiO_4$ on

© 2017 The Japan Society of Applied Physics

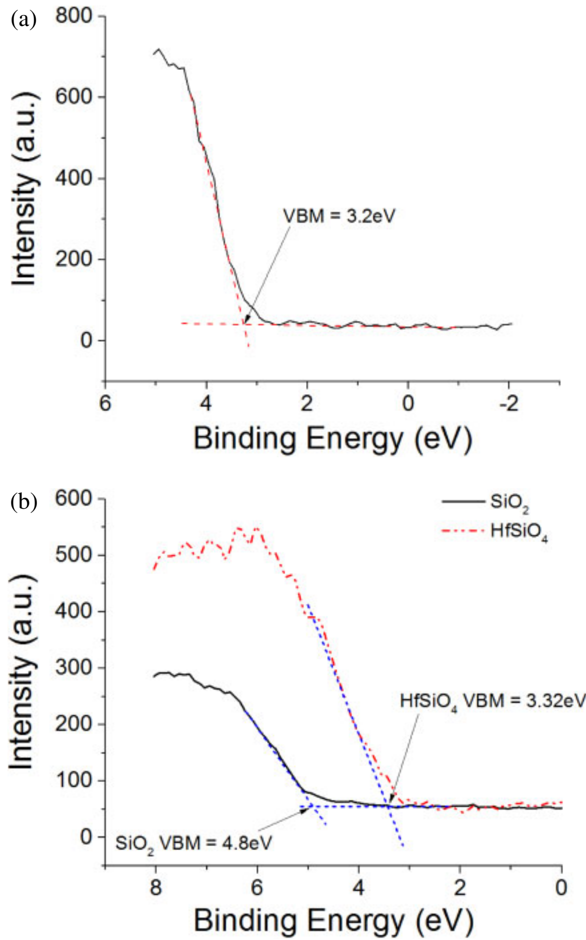

Fig. 2. (Color online) XPS spectra of core levels to VBM for bulk Ga_2O_3 (a) and thick film SiO_2 and $HfSiO_4$ deposited by ALD (b). The intensity is in arbitrary units (a.u.).

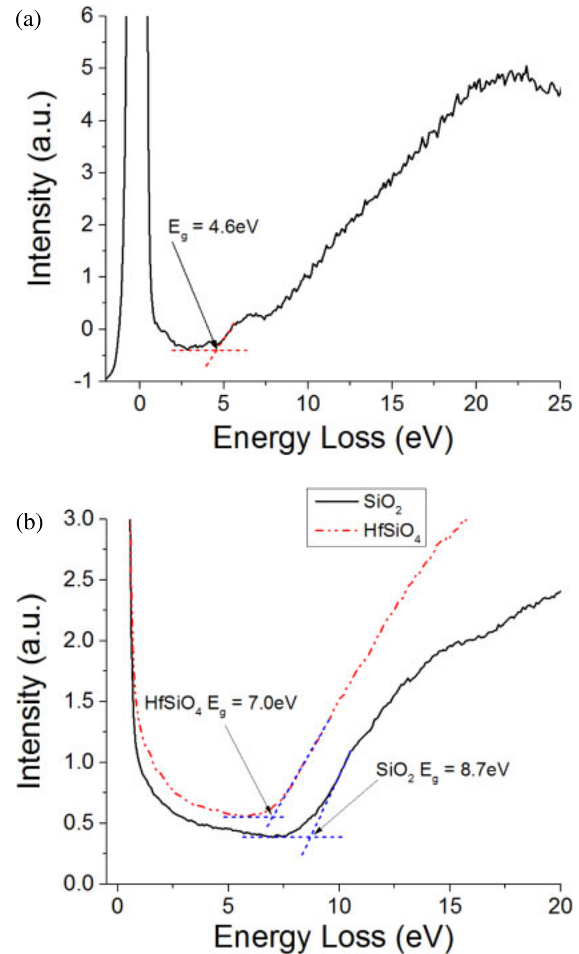

Fig. 3. (Color online) (a) Reflection electron energy loss spectra to determine the bandgap of bulk Ga_2O_3 and (b) for thick film SiO_2 and $HfSiO_4$ deposited by ALD. The intensity is in arbitrary units (a.u.).

β-Ga_2O_3 and finally, the bulk β-Ga_2O_3 crystals. The spectra are free from contaminants and consistent with past published XPS data on these materials.[22,27] In particular, we looked carefully for the presence of metallic contaminants in the films whose oxides might lower the overall bandgap of the dielectrics and thus affect the band alignment. However these were not detected to the sensitivity level of XPS.

The valence band maximum (VBM) was determined by linearly fitting the leading edge of the valence band and the flat energy distribution from the XPS measurements, and finding the intersection of these two lines,[23,24] as shown in Fig. 2 for the bulk β-Ga_2O_3 (a) and thick SiO_2 and $HfSiO_4$ (b). The VBM was measured to be 3.2 ± 0.2 eV for β-Ga_2O_3, which is consistent with previous reports[14–21,27] and 4.8 ± 0.4 eV for the SiO_2 or 3.32 ± 0.3 eV for the $HfSiO_4$.

The bandgap of the β-Ga_2O_3 was determined to be 4.6 ± 0.3 eV, as shown in the REELS spectra in Fig. 3(a). The band gap was determined from the onset of the energy loss spectrum.[26] The measured band gap for the SiO_2 was 8.7 ± 0.4 eV from the REELS data of Fig. 3(b). Both of these numbers are consistent with literature values and are identical to those reported by Konishi et al.[15] The bandgap for $HfSiO_4$ was found to be 7.0 ± 0.3 eV. The difference in bandgaps between SiO_2 and β-Ga_2O_3 is therefore 4.1 eV and between $HfSiO_4$ and β-Ga_2O_3 is 2.4 eV. To determine the actual band alignment and the respective valence and conduction band offsets, we examined the core level spectra for the samples.

High resolution XPS spectra of the VBM-core delta region are shown in Fig. 4 for the β-Ga_2O_3 (a) and thick ALD SiO_2 and $HfSiO_4$ (b) samples. These were used to determine the selected core level peak positions. Figure 5 shows the XPS spectra for the β-Ga_2O_3 to SiO_2 and β-Ga_2O_3 to $HfSiO_4$ core delta regions of the two types of heterostructure samples. These values are summarized in Table II for the two heterostructures examined and these were then inserted into the following equation to calculate ΔE_V:[24,25]

$$\Delta E_V = (E_{Core} - E_{VBM})_{Ref_Ga_2O_3} - (E_{Core} - E_{VBM})_{Ref_dielectric} - (E^{Ga_2O_3}_{Core} - E^{dielectric}_{Core})^{dielectric}_{Ga_2O_3}$$

In this equation the core parameters refer to either Si 2p or Ga $2p_{3/2}$ when measuring the dielectric or β-Ga_2O_3 spectra, respectively. The reference Ga_2O_3 refers to the bulk β-Ga_2O_3 and the reference dielectric refers to the thick SiO_2 or $HfSiO_4$ films.

Figure 6 shows the band diagrams of the SiO_2/β-Ga_2O_3 and $HfSiO_4$/β-Ga_2O_3 heterostructures. Our data shows the alignments are both nested, type I alignments with a valence band offset of 1.23 ± 0.2 eV and conduction band offset of 2.87 ± 0.4 eV for the SiO_2/β-Ga_2O_3 system using the following equation: $\Delta E_C = E_g^{SiO_2} - E_g^{Ga_2O_3} - \Delta E_V$, i.e., $\Delta E_C = 8.7$ eV − 4.6 eV − 1.23 eV = 2.87 eV. The corresponding values for the $HfSiO_4$/β-Ga_2O_3 are $\Delta E_V = 0.02$ eV and $\Delta E_C = 2.38$ eV. The valence band offset is too small to provide

© 2017 The Japan Society of Applied Physics

Table II. Summary of measured core levels in these experiments (eV).

Reference Ga_2O_3				Reference dielectric				Thin dielectric on Ga_2O_3	
Ga_2O_3 metal core	Ga_2O_3 VBM	Metal core level	Metal core-Ga_2O_3 VBM	Film	Dielectric VBM	Si 2p core level	Si 2p–VBM	DCL Ga $2p_{3/2}$–Si 2p	Valence band offset
Ga $2p_{3/2}$	3.20	1118.10	1114.90	SiO_2	4.80	103.40	98.60	1015.07	1.23
				$HfSiO_4$	3.32	102.30	98.98	1015.90	0.02

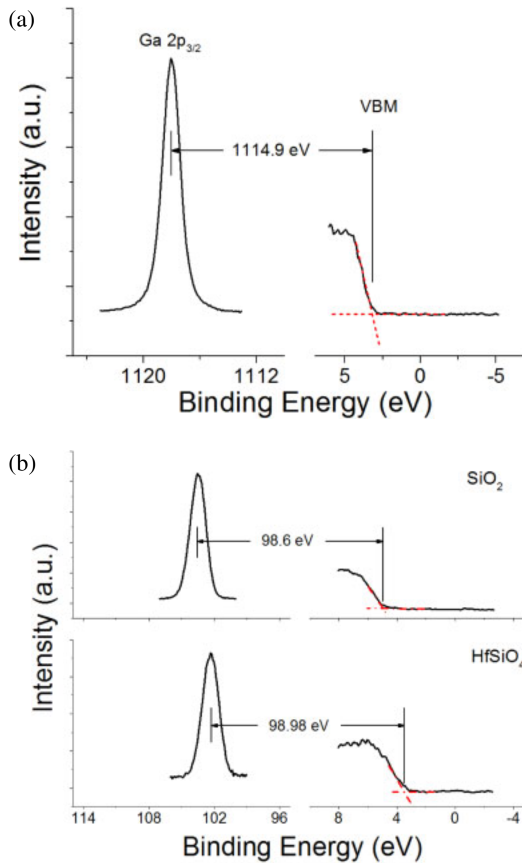

Fig. 4. (Color online) High resolution XPS spectra for the vacuum-core delta regions of (a) the bulk Ga_2O_3 (a) and ALD SiO_2 and $HfSiO_4$ (b). The intensity is in arbitrary units (a.u.).

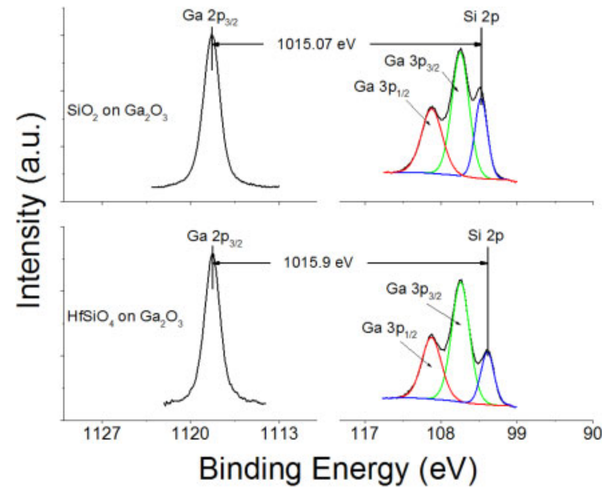

Fig. 5. (Color online) High resolution XPS spectra for the Ga_2O_3 to SiO_2 and $HfSiO_4$-core delta regions. The intensity is in arbitrary units (a.u.).

$$\Delta E_C = E_g^{Dielectric} - E_g^{Ga_2O_3} - \Delta E_V$$

$$\Delta E_C(SiO_2) = 8.7eV - 4.6eV - 1.23eV = \mathbf{2.87eV}$$

$$\Delta E_C(HfSiO_4) = 7.0eV - 4.6eV - 0.02eV = \mathbf{2.38eV}$$

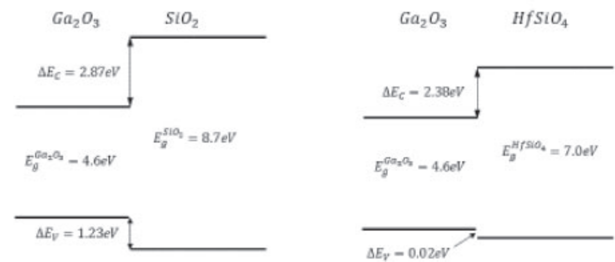

Fig. 6. Band diagrams for SiO_2/Ga_2O_3 and $HfSiO_4/Ga_2O_3$ heterostructures in which the dielectrics were deposited by ALD. The valence band offset was determined to be 1.23 ± 0.20 eV for ALD SiO_2 on β-Ga_2O_3 and 0.02 ± 0.003 eV for $HfSiO_4$. The respective conduction band offsets were 2.87 ± 0.70 eV for ALD SiO_2 and 2.38 ± 0.50 eV for $HfSiO_4$, respectively.

effective hole confinement, but this material might still be a candidate as a surface passivation layer for Ga_2O_3.

The literature on band alignments in all dielectric/semiconductor systems shows that energy band alignment variations of sometimes more than 1 eV depending on interface preparation can be obtained,[28–35] due to the presence of high defect concentrations in the materials and on a cation effect that will increase the VBM of that material. These differences are usually seen for the same heterostructure but different deposition methods, i.e., sputtering is more prone to creating interfacial disorder and also have metallic contamination that affects the bandgap of the dielectric.[31–33] The literature on band alignments on β-Ga_2O_3 is not yet extensive enough to draw those conclusions for that system. Our data on SiO_2 is the same as that of Konishi et al.[15] within the experimental error. In their case they used PECVD SiO_2. Our data is not as consistent with that of Jia et al.,[15] even though they used a nominally similar ALD process to deposit the SiO_2 on bulk, single-crystal β-Ga_2O_3. They also used capacitance–voltage measurements and showed consistency with their XPS data (conduction band offsets of 3.76 eV with the former, 3.63 eV with the latter). We have seen significant differences in band offsets for Al_2O_3 deposited by either sputtering or ALD[36] and these were in turn different from other reports of ALD Al_2O_3 on β-Ga_2O_3 by Kamimura et al.[16] They obtained a valence band offset of 0.7 eV for ALD Al_2O_3 on β-Ga_2O_3 using similar deposition conditions to those used in our work. They showed the presence of a significant density of border traps in their Al_2O_3 from capacitance–voltage data,[16] but the differences with our results show that even nominally similar dielectric deposition conditions can still lead to variations in reported band alignments. This is emphasized by the results

© 2017 The Japan Society of Applied Physics

of Jia et al.[14] with a valence band offset of 0.43 eV compared to the 1.2 eV determined here even though the dielectric was deposited by ALD in both cases. Table I shows that SiO_2 is the best choice as a gate dielectric on β-Ga_2O_3 of the materials investigated to date, since it has large conduction and valence band offsets.

4. Summary and conclusions

The band alignment at SiO_2/β-Ga_2O_3 and $HfSiO_4/\beta$-Ga_2O_3 heterojunctions was obtained from XPS measurements and in both cases were found to be nested gap (type I) band offsets. For SiO_2 the valence band offset was 1.2 eV and the conduction band offset was 2.9 eV, while for $HfSiO_4$ the valence band offset was 0.02 eV and the conduction band offset was 2.38 eV. The conduction band offsets in both cases are large and provide excellent electron confinement, but the valence band offset for $HfSiO_4$ is too small for limiting hole transport. A comparison of the literature to date on band offsets for dielectrics on β-Ga_2O_3 shows that SiO_2 is the best choice. Our data for SiO_2 on β-Ga_2O_3 is consistent with the report from Konishi et al.[15] who employed PECVD SiO_2 in their work.

Acknowledgments

The project or effort depicted was also sponsored by the Department of the Defense, Defense Threat Reduction Agency, HDTRA1-17-1-011, monitored by Jacob Calkins. The content of the information does not necessarily reflect the position or the policy of the federal government, and no official endorsement should be inferred. The research at Dankook was supported by the Basic Science Research Program through the National Research Foundation of Korea (NRF) funded by the Ministry of Education (2014R1A1A4A01008877, 2015R1D1A1A01058663), and Nano Material Technology Development Program through the National Research Foundation of Korea (NRF) funded by the Ministry of Science, ICT and Future Planning (2015M3A7B7045185). Part of the work at Tamura Corporation was supported by "The research and development project for innovation technique of energy conservation" of the New Energy and Industrial Technology Development Organization (NEDO), Japan. We also thank Dr. Kohei Sasaki from Tamura Corporation for fruitful discussions.

1) A. Kuramata, K. Koshi, S. Watanabe, Y. Yamaoka, T. Masui, and S. Yamakoshi, Jpn. J. Appl. Phys. **55**, 1202A2 (2016).
2) Z. Galazka, R. Uecker, D. Klimm, K. Irmscher, M. Naumann, M. Pietsch, A. Kwasniewski, R. Bertram, S. Ganschow, and M. Bickermann, ECS J. Solid State Sci. Technol. **6**, Q3007 (2017).
3) M. Baldini, M. Albrecht, A. Fiedler, K. Irmscher, R. Schewski, and G. Wagner, ECS J. Solid State Sci. Technol. **6**, Q3040 (2017).
4) M. Higashiwaki, K. Sasaki, H. Murakami, Y. Kumagai, A. Koukitu, A. Kuramata, T. Masui, and S. Yamakosh, Semicond. Sci. Technol. **31**, 034001 (2016).
5) S. Oh, J. Kim, F. Ren, S. J. Pearton, and J. Kim, J. Mater. Chem. C **4**, 9245 (2016).
6) K. D. Chabak, N. Moser, A. J. Green, D. E. Walker, Jr., S. E. Tetlak, E. Heller, A. Crespo, R. Fitch, J. P. McCandless, K. Leedy, M. Baldini, G. Wagner, Z. Galazka, X. Li, and G. Jessen, Appl. Phys. Lett. **109**, 213501 (2016).
7) A. J. Green, K. D. Chabak, E. R. Heller, R. C. Fitch, Jr., M. Baldini, A. Fiedler, K. Irmscher, G. Wagner, Z. Galazka, S. E. Tetlak, A. Crespo, K. Leedy, and G. H. Jessen, IEEE Electron Device Lett. **37**, 902 (2016).
8) M. J. Tadjer, N. A. Mahadik, V. D. Wheeler, E. R. Glaser, L. Ruppalt, A. D. Koehler, K. D. Hobart, C. R. Eddy, Jr., and F. J. Kub, ECS J. Solid State Sci. Technol. **5**, P468 (2016).
9) M. Higashiwaki, K. Sasaki, T. Kamimura, M. H. Wong, D. Krishnamurthy, A. Kuramata, T. Masui, and S. Yamakoshi, Appl. Phys. Lett. **103**, 123511 (2013).
10) K. Konishi, K. Goto, H. Murakami, Y. Kumagai, A. Kuramata, S. Yamakoshi, and M. Higashiwaki, Appl. Phys. Lett. **110**, 103506 (2017).
11) W. S. Hwang, A. Verma, H. Peelaers, V. Protasenko, S. Rouvimov, H. (Grace) Xing, A. Seabaugh, W. Haensch, C. Van de Walle, Z. Galazka, M. Albrecht, R. Fornari, and D. Jena, Appl. Phys. Lett. **104**, 203111 (2014).
12) S. Ahn, F. Ren, J. Kim, S. Oh, J. Kim, M. A. Mastro, and S. J. Pearton, Appl. Phys. Lett. **109**, 062102 (2016).
13) J. Kim, S. Oh, M. Mastro, and J. Kim, Phys. Chem. Chem. Phys. **18**, 15760 (2016).
14) Y. Jia, K. Zheng, J. S. Wallace, J. A. Gardella, and U. Singisetti, Appl. Phys. Lett. **106**, 102107 (2015).
15) K. Konishi, T. Kamimura, M. H. Wong, K. Sasaki, A. Kuramata, S. Yamakoshi, and M. Higashiwaki, Phys. Status Solidi B **253**, 623 (2016).
16) T. Kamimura, K. Sasaki, M. H. Wong, D. Krishnamurthy, A. Kuramata, T. Masui, S. Yamakoshi, and M. Higashiwaki, Appl. Phys. Lett. **104**, 192104 (2014).
17) M. Hattori, T. Oshima, R. Wakabayashi, K. Yoshimatsu, K. Sasaki, T. Masui, A. Kuramata, S. Yamakoshi, K. Horiba, H. Kumigashira, and A. Ohtomo, Jpn. J. Appl. Phys. **55**, 1202B6 (2016).
18) V. D. Wheeler, D. I. Shahin, M. J. Tadjer, and C. R. Eddy, Jr., ECS J. Solid State Sci. Technol. **6**, Q3052 (2017).
19) W. Wei, Z. Qin, S. Fan, Z. Li, K. Shi, Q. Zhu, and G. Zhang, Nanoscale Res. Lett. **7**, 562 (2012).
20) S. H. Chang, Z. Z. Chen, W. Huang, X. C. Liu, B. Y. Chen, Z. Z. Li, and E. W. Shi, Chin. Phys. B **20**, 116101 (2011).
21) Z. Chen, K. Hishihagi, X. Wang, K. Saito, T. Tanaka, M. Nishio, M. Arita, and Q. Guo, Appl. Phys. Lett. **109**, 102106 (2016).
22) D. C. Hays, B. P. Gila, S. J. Pearton, A. Trucco, R. Thorpe, and F. Ren, J. Vac. Sci. Technol. B **35**, 011206 (2017).
23) D. C. Hays, B. P. Gila, S. J. Pearton, and F. Ren, Appl. Phys. Rev. **4**, 021301 (2017).
24) E. A. Kraut, R. W. Grant, J. R. Waldrop, and S. P. Kowalczyk, Phys. Rev. Lett. **44**, 1620 (1980).
25) E. Bersch, M. Di, S. Consiglio, R. D. Clark, G. J. Leusink, and A. C. Diebold, J. Appl. Phys. **107**, 043702 (2010).
26) H. C. Shin, D. Tahir, S. Seo, Y. R. Denny, S. K. Oh, H. J. Kang, S. Heo, J. G. Chung, J. C. Lee, and S. Tougaard, Surf. Interface Anal. **44**, 623 (2012).
27) P. H. Carey, IV, F. Ren, D. C. Hays, B. P. Gila, S. J. Pearton, S. Jang, and A. Kuramata, Vacuum **141**, 103 (2017).
28) X. Guo, H. Zheng, S. W. King, V. V. Afanas'ev, M. R. Baklanov, J.-F. de Marneffe, Y. Nishi, and J. L. Shohet, Appl. Phys. Lett. **107**, 082903 (2015).
29) A. Zur and T. C. McGill, J. Vac. Sci. Technol. B **2**, 440 (1984).
30) H.-K. Dong and L.-B. Shi, Chin. Phys. Lett. **33**, 016101 (2016).
31) J. Xu, Y. Teng, and F. Teng, Sci. Rep. **6**, 32457 (2016).
32) M. Yang, R. Q. Wu, Q. Chen, W. S. Deng, Y. P. Feng, J. W. Chai, J. S. Pan, and S. J. Wang, Appl. Phys. Lett. **94**, 142903 (2009).
33) A. Klein, J. Phys.: Condens. Matter **27**, 134201 (2015).
34) A. Klein, Thin Solid Films **520**, 3721 (2012).
35) S. Li, F. Chen, R. Schafranek, T. J. M. Bayer, K. Rachut, A. Fuchs, S. Siol, M. Weidner, M. Hohmann, V. Pfeifer, J. Morasch, C. Ghinea, E. Arveux, R. Gunzler, J. Gassmann, C. Korber, Y. Gassenbauer, F. Sauberlich, G. V. Rao, S. Payan, M. Maglione, C. Chirila, L. Pintilie, L. Jia, K. Ellmer, M. Naderer, K. Reichmann, U. Bottger, S. Schmelzer, R. C. Frunza, H. Ursic, B. Malic, W.-B. Wu, P. Erhart, and A. Klein, Phys. Status Solidi: Rapid Res. Lett. **8**, 571 (2014).
36) P. H. Carey, F. Ren, D. C. Hays, B. P. Gila, S. J. Pearton, S. Jang, and A. Kuramata, Vacuum **142**, 52 (2017).

© 2017 The Japan Society of Applied Physics

View publication stats